

Growth and characterization of $(K_{0.5} Na_{0.5})NbO_3$ thin films by a sol–gel method

Chiwon Kang · Jung-Hyun Park · Dongna Shen ·
Hosang Ahn · Minseo Park · Dong-Joo Kim

Received: 23 June 2010/Accepted: 4 November 2010/Published online: 17 November 2010
© Springer Science+Business Media, LLC 2010

Abstract $(K_{0.5} Na_{0.5})NbO_3$ (KNN) perovskite materials have been developed as a promising lead-free piezoelectric material for environmentally benign piezoelectric devices. KNN films with about 320 nm thickness were fabricated on Pt(111)/SiO₂/Si(100) substrates by a sol–gel method from stoichiometric and A-site ion excess precursor solutions. Two different annealing methods were also used to investigate the crystallographic evolution of the films. A layer-by-layer annealing process results in highly (001) oriented KNN from the annealing temperature of 550 °C, while the final annealing method leads to weaker crystalline peaks with a random orientation. The KNN films from the K and Na excess precursor solutions show similar crystallization behavior. However, the ferroelectric hysteresis loops of the films were greatly improved by compensating for an A-site vacancy. In particular, the KNN films from K-excess precursor solutions show better ferroelectric properties compared to the films prepared from Na excess solutions.

Keywords $(K_{0.5} Na_{0.5})NbO_3$ · Piezoelectric material · Thin film · Crystallization

C. Kang · J.-H. Park · D. Shen · H. Ahn · D.-J. Kim (✉)
Materials Research and Education Center, Auburn University,
275 Wilmore Labs, Auburn, AL 36849-5341, USA
e-mail: dkim@eng.auburn.edu

M. Park
Department of Physics, Auburn University, Auburn, AL 36849,
USA

1 Introduction

Many lead-free piezoelectric materials such as Bi-based compounds, BaTiO₃, or alkaline niobate compounds have been intensively studied due to ecological issues [1–3]. Alkaline niobate-based compounds, especially $(K_{0.5} Na_{0.5})NbO_3$ (KNN), are currently being considered as one of the promising lead-free piezoelectric materials due to their relatively good piezoelectricity and a high Curie point [1–3]. In addition, KNN is known to form a solid solution of ferroelectric KNbO₃ and antiferroelectric NaNbO₃ similar to the PZT system [4], which spurs the development of commercial compositions and optimizes the processing in order to obtain reproducible properties.

Thin and thick film processing of piezoelectric materials is necessary to apply KNN materials in many microelectromechanical systems driven by miniaturization and integration [5, 6]. Growth of KNN-based thin films has been investigated by several methods such as pulsed laser deposition (PLD) [7], aerosol deposited films [8], metal organic chemical vapor deposition [9], radio frequency (rf) magnetron sputtering [10, 11], and chemical solution deposition (CSD) [12–15]. The CSD method, such as the sol–gel process, is divided in several steps: solution synthesis, coating on a substrate, pyrolysis, and subsequent crystallization process. Compared to the physical methods such as sputtering or PLD, the CSD process of a multi-precursor enables a higher homogeneity at the molecular level and allows for synthesis at a lower temperature. Several results showed the use of the sol–gel process to fabricate KNN thin films. However, to date, there are still few reports on the properties of KNN thin films by the sol–gel process and their relationships with processing parameters.

In this work, several sol-gel processing parameters in the fabrication of KNN thin films on Pt(111)/SiO₂/Si(100) were investigated. Thermal analysis of the KNN gel powders was performed to examine the progressive stages of organic combustion and the subsequent crystallization of the KNN thin film. The crystallization behavior and microstructure of the KNN thin films were investigated by varying annealing methods. The ferroelectric properties of the KNN thin films were also characterized depending on annealing temperature and the stoichiometry of the precursor solutions.

2 Experimental procedure

(K_{0.5} Na_{0.5})NbO₃ (KNN) solution was fabricated by dissolving Na-ethoxide (Sigma-Aldrich, 95%), K-ethoxide (Sigma-Aldrich, 95%), and Nb-pentaethoxide (Sigma-Aldrich, 99.95%) as sol-gel precursors in 2-methoxyethanol (Sigma-Aldrich, ≥99.9%) and acetylacetone (Sigma-Aldrich, ≥99%), respectively as the solvent and chelating agent. The KNN solution was prepared under a dry nitrogen atmosphere, and the process step is as follows: Nb-pentaethoxide was added in 2-methoxyethanol and stirred for 1 h at 80 °C. Subsequently, K-ethoxide was dissolved into the Nb-alkoxide solution and stirred for 1 h at 80 °C. Finally, Na-ethoxide was added to the Nb-, K-alkoxide solution and stirred for 1 h at 80 °C. The mixed solution was adjusted to yield a homogeneous concentration of 0.3 M. For preparing K and/or Na excess solutions, the (Na + K)/Nb ratio was kept to 1.1, and three different excess conditions, 10 mol% K, 5 mol% Na and 5 mol% K, and 10 mol% Na excess precursor solutions, were prepared. After preparation, the solution was spin-coated on 15 × 15 mm² Pt(111)/SiO₂/Si(100) substrates in air at 3,000 rpm for 30 s. The deposited films were subsequently dried for 8 min at 150 °C on a hot plate for their chemical stabilization. Promptly after drying, the gel films were pyrolyzed for 10 min at 350 °C to remove organic residues. Finally, the films were annealed for 2 min in air at either 450, 550, 650, or 750 °C (called a layer-by-layer annealing process). The coating process was repeated 15 times and the total thickness was about 320 nm. In addition, to study the influence of the pyrolyzed layer thickness on the crystallization, a buildup of pyrolyzed layers before annealing was obtained by repeating the above mentioned processes 15 times (without annealing) for KNN on Pt(111)/SiO₂/Si(100) substrate. Following pyrolysis, the KNN thin films were annealed for 1 h in air with a ramp of 5 °C/min (called final annealing process).

The powders prepared by drying the KNN sol-gel precursors at 50 °C were thermally analyzed using differential scanning calorimetry—thermogravimetry (DSC-TG, TA).

The crystalline phases of the KNN thin films were characterized by X-ray diffraction (XRD) using a Rigaku Miniflex powder X-ray diffractometer with Cu K α radiation. Micro-Raman spectroscopy (Jobin-Yvon) with 441.6 nm laser lines from a He-Cd laser (Kimmon Electric) was also utilized for the crystallinity study. The microstructure was observed by using a field-emission scanning electron microscope (FE-SEM, JEOL). The ferroelectric properties were analyzed by using a ferroelectric tester (aixACCT Systems, TF 2000).

3 Results and discussion

The solution system was analyzed to investigate the types of bonding and to determine heat treatment conditions for thin film synthesis. Figure 1 illustrates the results of differential scanning calorimetry (DSC) and the thermogravimetric analysis (TGA) curves of the KNN precursor gel powders dried at 50 °C. The weight of the powder gel rapidly decreased until around 90 °C where a large endothermic peak emerged. This peak is associated with the evaporation of the water contained in the gel. The peak at 335 °C may be caused by decomposition of metal alkoxides and hydrocarbons. The peak at 500 °C may arise from the combustion of residual carbon. The gradual loss in weight about 28.1% until 500 °C was measured. The strongest peak at 550 °C can be due to the crystallization of the KNN because there is no corresponding weight loss in the TGA curve. Therefore, the annealing temperature was chosen from around 500 °C. To obtain crack-free films, much of the attention should be given in the pyrolysis procedure in the range about 90–350 °C since severe weight loss can occur in this temperature range. From the results, a three-step heat treatment (low temperature drying at 150 °C, medium temperature pyrolysis at 350 °C, and annealing at the ranging from 450 to 750 °C) was employed to prepare dense and crack-free films. Different stoichiometric precursors such as Na and/or K excess precursor solutions were also characterized. However, DSC-TG results do not show a difference depending on the stoichiometry of the precursors.

To investigate the effects of annealing temperature on the crystallization, the XRD patterns of KNN thin films on Pt(111)/SiO₂/Si(100) substrates were observed as shown in Fig. 2. Crystalline phases began to appear from 550 °C and upward as seen in the (001) peaks at 22.5° and the (002) peaks at 46.1°, very close to the temperature estimated from DSC-TG. With increasing annealing temperature, the intensities of the (001) and (002) peaks increased corresponding to the enhanced crystallinity. KNN bulk ceramics are known to have an orthorhombic structure at room temperature, and lattice parameters of the bulk KNN

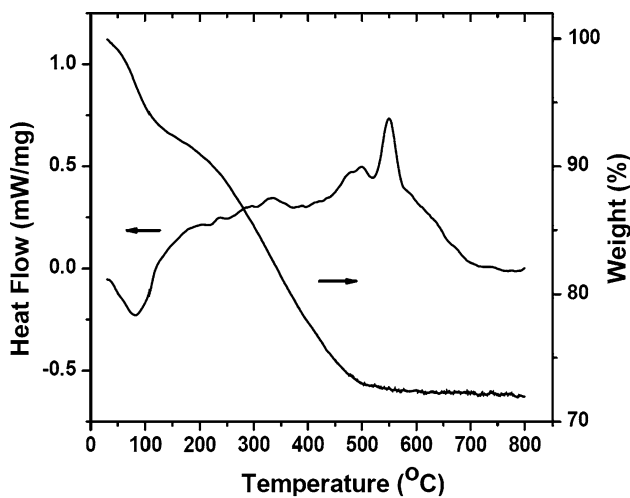


Fig. 1 DSC-TG curves of the $(\text{K}_{0.5} \text{Na}_{0.5})\text{NbO}_3$ dried gel powders heated in air at $10 \text{ }^{\circ}\text{C}/\text{min}$

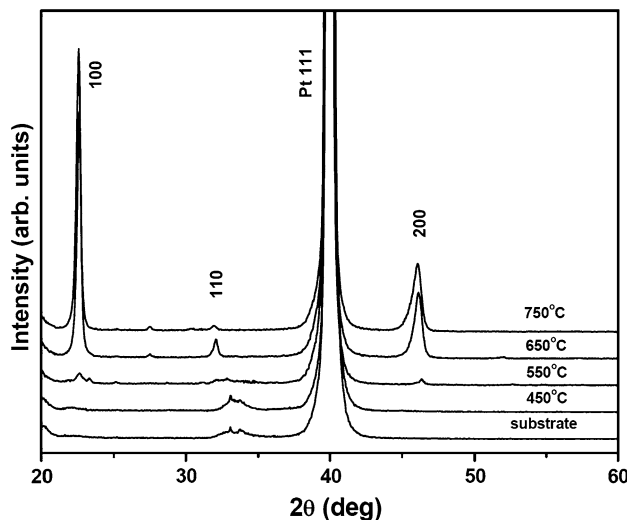


Fig. 2 XRD patterns of the KNN thin films fabricated by a layer-by-layer annealing process ranging from 450 to $750 \text{ }^{\circ}\text{C}$ on Pt(111)/SiO₂/Si(100) substrates

($a = 0.3994 \text{ nm}$, $b = 0.4016 \text{ nm}$ and $c = 0.3935 \text{ nm}$) were reported by Singh et al. [4]. However, the peaks of these KNN thin films did not split. By assuming KNN thin films have a pseudo-cubic structure, the calculated lattice parameter of KNN annealed at $750 \text{ }^{\circ}\text{C}$ was approximately in the range of 0.393 – 0.396 nm based on the peaks that appeared at 22.5° , 32° , and 46.1° . This result was consistent with the earlier report [14]. A final annealing process was also conducted to investigate the KNN thin film crystallization. The effect of the thicker pyrolyzed layer on the crystallization was shown in Fig. 3. The films prepared by a final annealing method start to show distinct XRD peaks from $650 \text{ }^{\circ}\text{C}$, but the XRD peaks exhibit weaker peak intensities with a random orientation. For thicker

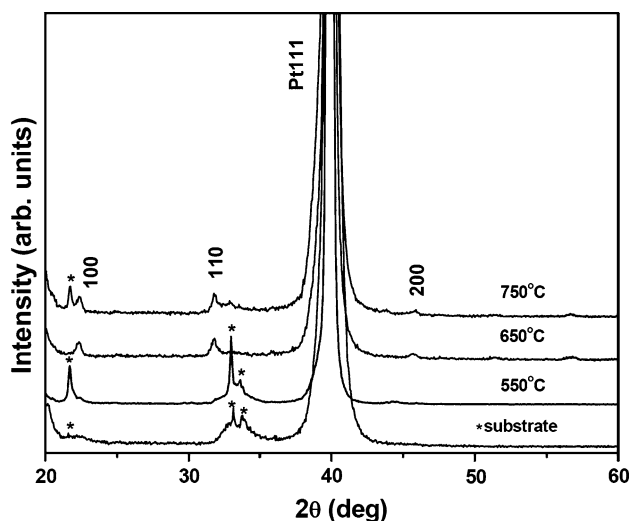


Fig. 3 XRD patterns of KNN films grown on Pt(111)/SiO₂/Si(100) by a final annealing process

pyrolyzed layers, the time required for the nucleation and growth of the interface-nucleated grains to reach the opposing surface would be greater than for thinner layers during annealing [16]. At higher temperatures, since the energy barriers will be sufficiently overcome, homogeneous nucleation and growth may easily occur inside of the thin films [17]. As a result, a random orientation similar to bulk KNN ceramics can be observed. Randomly oriented KNN films were commonly reported when a similar heat treatment like the final annealing method was adopted [12, 15]. Textured orientation with a uniform and controllable microstructure is an essential requirement for the improvement in electrical properties and for the device design. The KNN films prepared by the layer-by-layer process were only focused in this study.

In addition to X-ray analysis, micro-Raman spectroscopy was performed to further investigate the degree of crystallization of the KNN thin films. Figure 4 presents the Raman spectra of KNN thin films deposited on Pt(111)/SiO₂/Si(100) substrates, followed by annealing at different temperatures. Recently, Kakimoto et al. [18] has reported the Raman spectra of the $(\text{K}_{0.5} \text{Na}_{0.5})\text{NbO}_3$ powder. Our Raman spectra collected from the samples annealed at 650 and $750 \text{ }^{\circ}\text{C}$ exhibit similar features to those of the KNN powder. The peaks at around 245 , 550 and 610 cm^{-1} are attributed to ν_5 (E_{2g}), ν_2 (E_g) and ν_1 (A_{1g}) vibrational modes of NbO₆ octahedra, respectively. The peak at around 855 cm^{-1} corresponds to the combination mode of ν_1 (A_{1g}) and ν_5 (F_{2g}). As can be clearly seen from the figure, the Raman spectra collected from the samples annealed at 650 and $750 \text{ }^{\circ}\text{C}$ did not exhibit any substantial difference, which is consistent with the result obtained from the X-ray diffraction study. The Raman results imply that a crystallized phase starts to form when annealed at those temperatures.

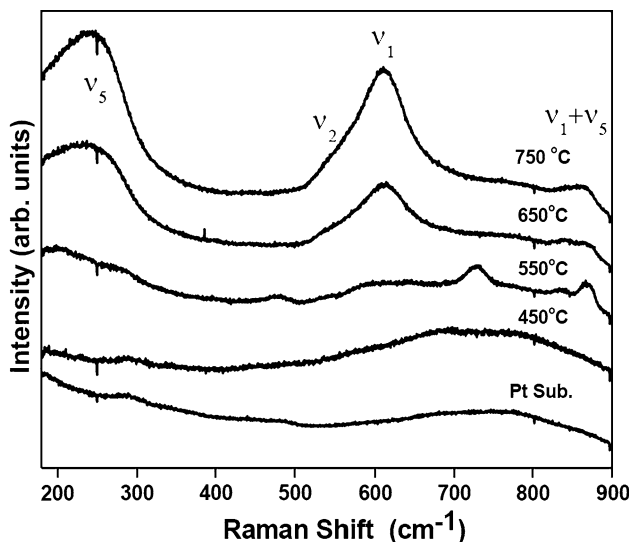


Fig. 4 Raman spectra of KNN thin films by a layer-by-layer annealing process at different annealing temperature

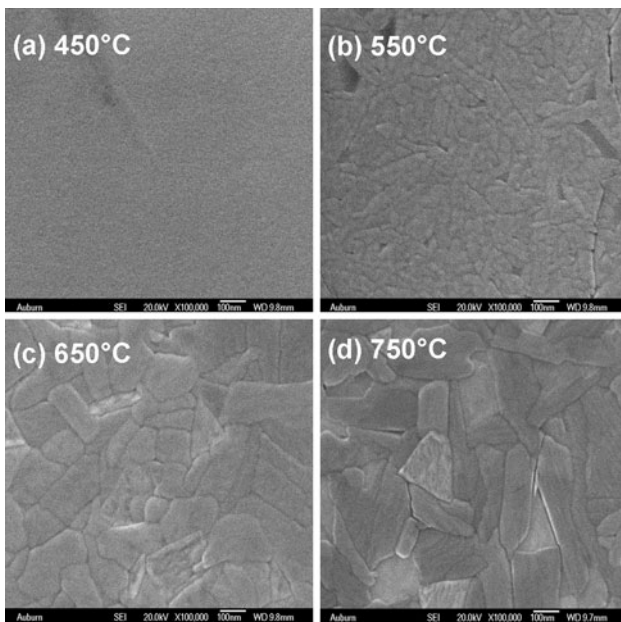


Fig. 5 SEM micrographs of the KNN thin films by a layer-by-layer annealing process at different annealing temperature on Pt(111)/SiO₂/Si(100) substrates

Figure 5 shows the microstructures of KNN thin films annealed at 450 to 750 °C. Microstructure evolution was strongly dependent on annealing temperatures, and the grains were clearly observed from the annealing temperature of 550 °C, indicating the beginning of crystallization in these films. In addition, the average grain size increased with an elevated annealing temperature as expected. Tanaka et al. reported the decrease of grain size at higher annealing temperature of 700 °C possibly due to

volatilization of alkaline elements [14], but our KNN films do not show such a distinct microstructure change. Figure 6 shows the P-E hysteresis loops of KNN thin films on Pt(111)/SiO₂/Si(100) substrates annealed at different temperatures. The P-E hysteresis loops of the KNN film annealed at 550 °C were round in shape and not completely saturated, indicating some leakage components in the films. Leaky behaviors become less significant with increasing annealing temperature. In case of the KNN thin film annealed at 750 °C, $2P_r$ and $2E_c$ values show 19 μ C/cm² and 200 kV/cm, respectively. It is likely that such incomplete saturation of the KNN films prepared from stoichiometric solutions can be attributed to the oxygen vacancies formed to maintain the charge neutrality in the KNN resulting by the loss of volatile Na and K.

To investigate the volatility effect of A-site cations, the amount of excessive K and/or Na in the sol-gel precursor solutions was varied, and the effects on film crystallinity were investigated by XRD. Although adding excess A-site ions might deteriorate the perovskite structures of KNN thin films, the KNN thin films prepared from K and/or Na excess precursor solutions still show the perovskite structure without distinct lattice distortion, as can be seen in Fig. 7. Also, there is no significant influence of excessive K and/or Na on the orientation, i.e. films from K and/or Na excess precursor solutions still show strong (001) orientation. P-E hysteresis loops of KNN thin films annealed at 750 °C were measured at different excess A-site solutions. Ferroelectric properties were clearly improved compared to the films synthesized by stoichiometric sol-gel precursors as shown in Fig. 8. The excess Na and K in the solution can compensate for the volatile ones during annealing and suppress the formation of the oxygen vacancies. As a result, reasonably saturated P-E hysteresis loops can be created. When comparing the effects of K and Na, it appears that the K excess solution is effective for the ferroelectric properties. The KNN films prepared by the 10 mol% K excess precursor solution present better saturation behavior. The polarization values of the KNN films increased in the order: 10 mol% excess Na, 5 mol% K and 5 mol% Na excess, 10 mol% K excess solution. Lee et al. reported a more volatile nature of K in solid state sintered KNN ceramics [19]. Higher performance of KNN films from K excess precursor solution may be due to different bonding affinity between alkaline elements and the gel network, which may influence the volatility during the heat treatment process.

4 Conclusions

Lead-free piezoelectric ($K_{0.5}Na_{0.5}NbO_3$) (KNN) thin films were fabricated by a sol-gel method. Crystalline KNN thin

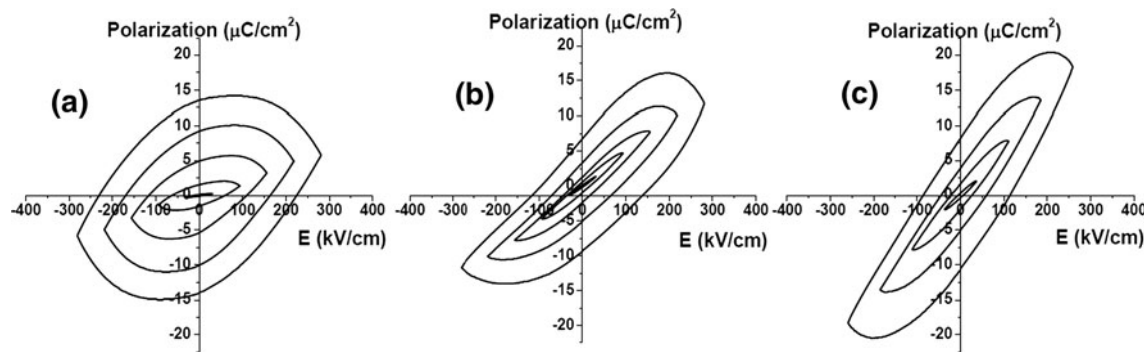


Fig. 6 Ferroelectric P-E hysteresis loops for KNN thin films fabricated from the stoichiometric sol-gel precursor solutions. Annealing temperatures for each sample are **a** 550 °C, **b** 650 °C, and **c** 750 °C, respectively

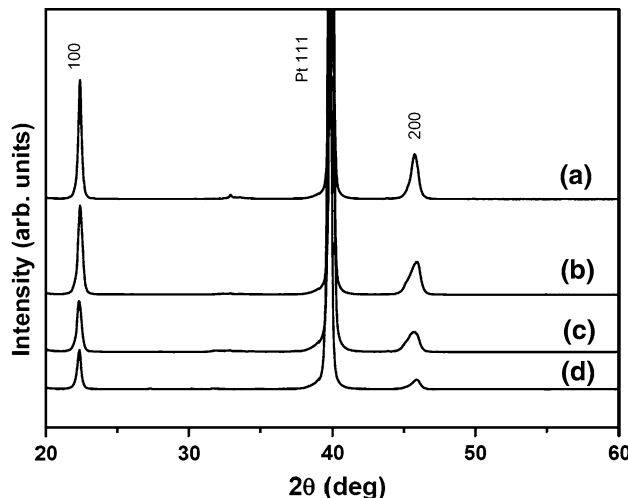


Fig. 7 XRD patterns of the KNN thin films on Pt(111)/SiO₂/Si(100) substrates from precursor solutions with various K/Na excess precursor solutions (**a**) 10 mol% K excess, (**b**) 5 mol% K and 5 mol% Na excess, (**c**) 10 mol% Na excess, and (**d**) stoichiometric solution. (The annealing process was conducted by using a layer-by-layer annealing method at 750 °C for the comparison)

films with highly (001) orientation were grown from temperatures as low as 550 °C on Pt(111)/SiO₂/Si(100) substrates by the layer-by-layer annealing process. A final annealing method that influences the thickness of pyrolyzed film has a strong impact on the crystallization and orientation of these KNN films and results in weaker crystallinity with a random orientation. Although similar crystallization behavior was observed in the KNN films prepared from both stoichiometric and A-site excess precursor solutions, the excessive Na and K in the precursor solution is effective for better ferroelectric hysteresis loops. This result can be due to reduction of oxygen vacancies causing leaky behaviors. In addition, the KNN films prepared from K excess precursor solution show better ferroelectric hysteresis behavior compared to the films by Na excess solution.

Acknowledgments Parts of this work are supported by a research grant from the National Science Foundation (NSF-DMR-0605270) and by the Auburn University Detection and Food Safety Center (NIFA/USDA).

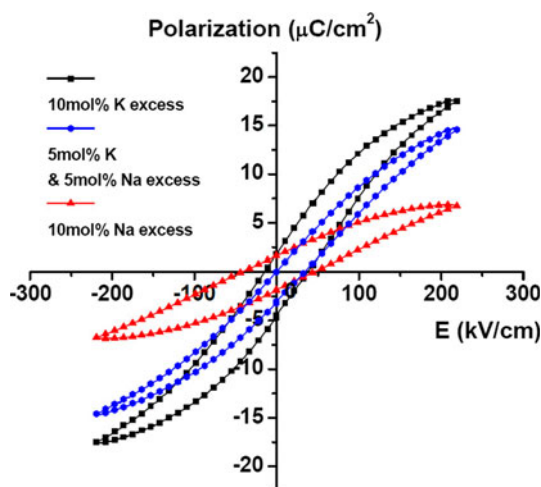


Fig. 8 The P-E hysteresis loops of the KNN thin films prepared from different Na and/or K excess precursor solutions

References

1. Saito Y, Takao H, Tani T, Nonoyama T, Takatori K, Homma T, Nagaya T, Nakamura M (2004) Nature 432:84–87
2. Maeder MD, Damjanovic D, Setter N (2004) J Electroceram 13:385–392
3. Rödel J, Jo W, Seifert TP, Anton E-M, Granzow T, Damjanovic D (2009) J Am Ceram Soc 92:1153–1177
4. Singh K, Lingwal V, Bhatt SC, Panwar NS, Semwal BS (2001) Mater Res Bull 36:2365–2374
5. Trolier-McKinstry S, Muralt P (2004) J Electroceram 12:7–17
6. Shen D, Park J-H, Ajitsaria J, Choe S-Y, Wikle HC, Kim D-J (2008) J Micromech Microeng 18(5):055017
7. Saito T, Wada T, Adachi H, Kanno I (2004) Jpn J Appl Phys 43(9B):6627–6631
8. Ryu J, Choi J-J, Hahn B-D, Park D-S, Yoon W-H, Kim K-H (2007) Appl Phys Lett 90(15):152901
9. Cho C-R (2002) Mater Lett 57(4):781–786
10. Khartsev SI, Grishin MA, Grishin AM (2005) Appl Phys Lett 86(6):062901

11. Kugler VM, Söderlind F, Music D, Helmersson U, Andreasson J, Lindbäck T (2004) *J Cryst Growth* 262:322–326
12. Lai F, Li F-F (2007) *J Sol-Gel Sci Technol* 42:287–292
13. Nakashima Y, Sakamoto W, Maiwa H, Shimura T, Yogo T (2007) *Jpn J Appl Phys* 46(14):L311–L313
14. Tanaka K, Kakimoto K-I, Ohsato H (2006) *J Cryst Growth* 294:209–213
15. Söderlind F, Käll P-O, Helmersson U (2005) *J Cryst Growth* 281:468–474
16. Meng XJ, Cheng JG, Sun JL, Tan J, Ye HJ, Chu JH (2000) *Thin Solid Films* 368(1):22–25
17. Yoon SH, Kim D-J (2007) *J Cryst Growth* 303:568–573
18. Kakimoto K-I, Akao K, Guo Y, Ohsato H (2005) *Jpn J Appl Phys* 44(9B):7064–7067
19. Lee Y-H, Cho J-H, Kim B-I, Choi D-K (2008) *Jpn J Appl Phys* 47(6):4620–4622